

# Role of Catalyst in Optimizing Fluid Catalytic Cracking Performance During Cracking of H-Oil-Derived Gas Oils

Dicho Stratiev,\* Ivelina Shishkova, Mihail Ivanov, Rosen Dinkov, Borislav Georgiev, Georgi Argirov, Vassia Atanassova, Petar Vassilev, Krassimir Atanassov, Dobromir Yordanov, Aleksey Popov, Alessia Padovani, Ulrike Hartmann, Stefan Brandt, Svetoslav Nenov, Sotir Sotirov, and Evdokia Sotirova



Cite This: *ACS Omega* 2021, 6, 7626–7637



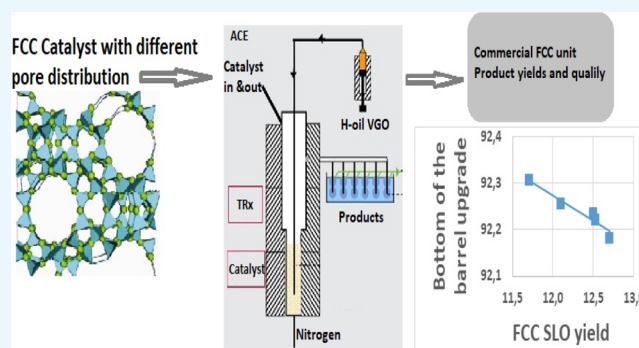
Read Online

ACCESS |

Metrics & More

Article Recommendations

**ABSTRACT:** Three H-Oil gas oils, heavy atmospheric gas oil (HAGO), light vacuum gas oil (LVGO), heavy vacuum gas oil (HVGO), and two their blends with hydrotreated straight run vacuum gas oils (HTSRVGOs) were cracked on two high unit cell size (UCS) lower porosity commercial catalysts and two low UCS higher porosity commercial catalysts. The cracking experiments were performed in an advanced cracking evaluation fluid catalytic cracking (FCC) laboratory unit at 527 °C, 30 s catalyst time on stream, and catalyst-to-oil (CTO) variation between 3.5 and 7.5 wt/wt. The two high UCS lower porosity catalysts were more active and more coke selective. However, the difference between conversion of the more active high UCS lower porosity and low UCS higher porosity catalysts at 7.5 wt/wt CTO decreased in the order 10% (HAGO) > 9% (LVGO) > 6% (HVGO) > 4% (80% HTSRVGO/20% H-Oil VGO). Therefore, the catalyst performance is feedstock-dependent. The four studied catalysts along with a blend of one of them with 2% ZSM-5 were examined in a commercially revamped UOP FCC VSS unit. The lower UCS higher porosity catalysts exhibited operation at a higher CTO ratio achieving a similar conversion level with more active higher UCS lower porosity catalysts. However, the higher UCS lower porosity catalysts made 0.67%  $\Delta$  coke that was higher than the maximum acceptable limit of 0.64% for this particular commercial FCC unit (FCCU), which required excluding the HVGO from the FCC feed blend. The catalyst system containing ZSM-5 increased the LPG yield but did not have an impact on gasoline octane. It was found that the predominant factor that controls refinery profitability related to the FCCU performance is the FCC slurry oil (bottoms) yield.



## INTRODUCTION

Since its introduction in 1942, fluid catalytic cracking (FCC) has become the main driver for oil refining performance improvement.<sup>1,2</sup> Over the years, it was found that FCC is a versatile process that can convert feeds of different origins—vacuum oils, residual oils, crude oil, scrap tires pyrolysis oil, polyethylene plastic waste, biomass derived oils—into high value transportation fuels and light olefin feeds for the petrochemical industry.<sup>3–9</sup> Among all independent variables which affect the FCC unit (FCCU) performance, the feedstock quality has the biggest impact.<sup>10–12</sup> While the processing of straight run vacuum gas oils (SRVGOs) in the FCCU is much more straightforward, the processing of secondary gas oils (from coker, visbreaker, and residue hydrocracker) is more challenging.<sup>13</sup> Secondary gas oils are indeed characterized by a higher basic nitrogen content and by a higher level of refractory condensed aromatic compounds.<sup>13–15</sup> The performance of the FCCU is therefore strictly correlated to the amount

and the quality of the secondary gas oil fraction present in the FCC feed blend.<sup>16,17</sup>

Fluid catalytic cracking is an acid-catalyzed process.<sup>18,19</sup> The modified zeolite Y in the FCC catalyst hereby contributes to most of the Brønsted acidity of the catalyst.<sup>19</sup> The Brønsted acidity contribution from the modified zeolite Y is a function of the zeolite content as well as its acid site density determined by the ratio of the silicon/alumina content of the zeolite. Acid site density of the modified zeolite Y is typically indicated by the unit cell size (UCS); the zeolite content is proportional to the microporous surface area, usually expressed as the zeolite surface area (ZSA). Both parameters could therefore be

Received: December 21, 2020

Accepted: February 25, 2021

Published: March 12, 2021

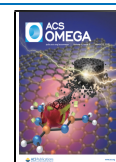


Table 1. Properties of the FCC Feeds Studied in This Work<sup>a</sup>

Nr		1	2	3	4	5
FCC feed properties	methods	feed 06.12.2018	feed 21.08.2019	H-Oil HVGO (11.4% FCC SLO in H-Oil feed) 26.03.2020	H-Oil LVGO (11.4% FCC SLO in H-Oil feed) 26.03.2020	H-Oil HAGO (11.4% FCC SLO in H-Oil feed) 26.03.2020
density at 15 °C, g/cm <sup>3</sup>	ASTM D4052	0.9101	0.916	0.9784	0.9639	0.9393
sulphur, wt %	ASTM D4294	0.29	0.27	0.67	0.48	0.37
nitrogen, wt %	ASTM D5762			0.25	0.32	0.21
basic nitrogen, mg/kg	UOP269	414	393	819	1070	686
Conradson carbon, wt %	ASTM D189	0.08	0.24	2.67	0.34	0.15
refractive index, 60 °C	ASTM D1747	1.493	1.499	1.551	1.540	1.521
C_Aromatics, wt %	ASTM D3238	23.3	24.4	41.3	43.6	38.7
C_Paraffins, wt %	ASTM D3238	61.2	60.1	48.6	47.6	50.7
C_Naphthenes, wt %	ASTM D3238	15.5	15.5	10.1	8.9	10.7
molecular weight, g/mol	VPO	387	396	416	323	296
sim. dist., °C	ASTM D2887-extended					
IBP		291	287	213	254	234
5% wt		350	353	395	316	300
10% wt		369	371	416	336	322
50%wt		436	444	484	403	373
90% wt		514	529	541	479	433
95% wt		533	556	556	503	455
FBP		588		595	555	517
Kw-factor		12.34	12.34	11.61	11.48	11.53
wt % H-Oil VGO in the FCC feed blend		22	20	100	100	100
H-Oil VGO density at 15 °C, g/cm <sup>3</sup>		0.956	0.956			
commercial FCCU conversion		75.2	74	ND	ND	ND

<sup>a</sup>ND = not determined.

considered as indicators for most of the Brønsted acidity of FCC catalyst particles. Besides the Brønsted acidity, Lewis acidity contributions play a role as well in the total acidity of FCC catalyst particles, and in this respect, the other FCC catalyst ingredients and processing play a significant role. Interested readers can refer to the extensive work of Velthoen<sup>19</sup> on the discussion of Lewis acidity in FCC catalysts.

The FCC catalyst's acid site density has a dominating impact in determining the selectivity of the catalyst. It is a crucial factor in designing catalysts for commercial application.<sup>20</sup>

Another governing factor in FCC catalyst design is the porosity of the FCC catalyst particle.<sup>21–29</sup> Diffusional effects have to be considered in FCC especially in the case of high molecular weight feed compounds like in secondary gas oils. It was found in our earlier research that the molecular weight of the H-Oil vacuum gas oils has a profound effect on coke and dry gas formation during their catalytic cracking,<sup>16</sup> highlighting the importance of diffusional limitations.

Since the start-up of the ebullated bed vacuum residue (VR) H-Oil hydrocracking in the LUKOIL Neftohim Burgas (LNB) refinery in the second half of 2015 whose generated VGO presents about one third of the feed for the FCCU, the FCC conversion started to vary from the initial 80–82 wt % ff, before commissioning the H-Oil, to 68 wt % ff depending on the amount and quality of the H-Oil VGO processed.<sup>16</sup> LNB

H-Oil VR hydrocracking is an ebullated bed hydrocracking technology, consisting of two ebullated bed reactors in series which convert vacuum residues from different origins on the supported NiMo catalyst in the conversion range 55–93 wt % ff.<sup>30,31</sup> The conversion in VR ebullated bed hydrocracking is thermally driven,<sup>32,33</sup> while the role of the catalyst is to supply hydrogen to the VR and prevent the formation of coke-like sediments<sup>33,34</sup> and remove impurities (sulfur, nitrogen, and metals). More information about the ebullated bed VR hydrocracking technology can be found in the literature.<sup>35,36</sup> About one third of the products of the H-Oil hydrocracker presents vacuum gas oil (VGO) whose quality variation depends on VR hydrocracking severity and the amount of processed FCC slurry oil (SLO) in the H-Oil feed blend.<sup>16,37,38</sup> The LNB H-Oil VGO consists of three streams: heavy atmospheric gas oil (HAGO), light vacuum gas oil (LVGO), and heavy vacuum gas oil (HVGO). The H-Oil VGO processing at the LNB FCCU consists of HAGO—20%; LVGO—30%; and HVGO—50% with the HVGO being the most problematic to the process.<sup>17</sup> The catalyst Δ coke that the LNB FCCU can tolerate is maximum 0.64 wt %. Beyond this, value regenerator temperature excursions go outside the safety limit set by the regenerator vessel design, that is 705 °C.<sup>16</sup> The catalyst was found to have a profound effect on the operation of the LNB FCCU. Therefore, selecting the most

suitable catalyst for a commercial FCCU that processes feed blends of primary (SRVGO) and secondary gas oils of variable quality and blend ratio represents a challenge. Moreover, the best method for catalyst selection is still a subject of debate. Catalysts can indeed be selected (1) on the basis of preliminary laboratory cracking experiments with the laboratory artificial deactivation of the fresh catalyst candidates or (2) on the basis of commercial tests with several catalyst candidates. The second option seems more risky, as it might result in significant loss of profit opportunities or deterioration of unit operation.<sup>39–41</sup>

In this study, we performed laboratory cracking experiments in an advanced cracking evaluation (ACE) unit with three pure H-Oil gas oils—HAGO = heavy atmospheric gas oil, LVGO = light vacuum gas oil, and HVGO = heavy vacuum gas oil. Three commercial FCC catalysts, which have been employed at the LNB FCCU, have been tested with three H-Oil gas oils.

Additionally, we carried out ACE tests with two FCC feeds sampled from the LNB FCCU on 18.12.2018 and 21.08.2019, consisting of 20 wt % H-Oil gas oils (10 wt % FCC SLO processed in the H-Oil VR hydrocracker) and 80 wt % SRVGO. These two LNB FCCU feeds were cracked on two commercial FCC catalysts.

Then, we compared the laboratory ACE results with the commercial LNB FCCU performance to evaluate the extent of similarity between the performance of ACE and the commercial FCCU while processing the same feed on the same catalysts. In the commercial LNB FCCU also, a catalytic system consisting of catalyst D plus 2 wt % ZSM-5 additive was employed to improve gasoline octane. The performance of that catalytic system was evaluated only in the commercial LNB FCCU.

The aim of this study is to outline the role of the selected catalyst technology in optimizing the commercial FCCU performance and to compare the conclusion from benchscale pilot plant testing to the commercial application and economics. To the best of our knowledge, this is the first time of spanning the evaluation of commercial catalysts from a laboratory scale to commercial scale and the resulting economic impact in the literature.

## RESULTS AND DISCUSSION

The physical–chemical properties of the FCC catalysts tested in the study are summarized in Table 2. With respect to catalysts C and G, catalyst B and D are characterized by a lower RE<sub>2</sub>O<sub>3</sub> content and higher total surface area (TSA). The UCS of the catalysts after deactivation indicates a lower acid site density for catalysts B and D compared to catalysts A and C which is in agreement with the lower RE<sub>2</sub>O<sub>3</sub> (rare earth oxides) content. Given the UCS, catalyst B and D would be expected to deliver higher LPG selectivity and lower gasoline selectivity compared to catalysts C and G.<sup>43</sup> Furthermore, catalyst B is characterized by a higher total and ZSA. The water and nitrogen accessible pore volumes are higher for catalyst B with respect to catalyst C and G indicating a higher porosity of catalyst B. The nitrogen pore volume distributions of catalysts B, C, and G are given in Figure 1.

Catalyst D is overall similar to catalyst B, in terms of the RE<sub>2</sub>O<sub>3</sub> content and UCS. Catalyst D has however lower TSA and lower pore volume. The nitrogen pore volume distributions of catalysts B and D are given in Figure 2.

Due to the distribution of fast and slow reacting species in the VGO, the kinetics of the catalytic cracking of VGO has

**Table 2. Properties of the Commercial FCC Catalyst Tested in This Study**

properties	catalyst B	catalyst C	catalyst G	catalyst D
	As Received			
Al <sub>2</sub> O <sub>3</sub> , wt %	40.3	43.0	40.5	41.9
RE <sub>2</sub> O <sub>3</sub> <sup>a</sup> , wt % (rare earth oxides)	1.4	2.6	2.7	1.6
Na <sub>2</sub> O, wt %	0.33	0.27	0.31	0.36
TSA, m <sup>2</sup> /g	335	278	301	311
ZSA, m <sup>2</sup> /g	290	237	260	262
matrix surface area, m <sup>2</sup> /g	45	41	41	49
	Deactivated (Metals-Free) <sup>b</sup>			
total surface area, m <sup>2</sup> /g	206	171	187	185
ZSA, m <sup>2</sup> /g	171	143	158	153
matrix surface area, m <sup>2</sup> /g	35	28	29	32
UCS, Å	24.26	24.31	24.31	24.26
PV N <sub>2</sub> , cm <sup>3</sup> /g	0.145	0.122	0.128	0.147
PV H <sub>2</sub> O, cm <sup>3</sup> /g	0.44	0.36	0.38	0.39
microactivity, wt % ff (at constant C/O) <sup>c</sup>	72	75	75	72

<sup>a</sup>Rare earth (RE) oxide content. <sup>b</sup>Deactivated (metals-free) catalyst properties means properties of the catalyst after laboratory artificial steam catalyst deactivation without impregnation with metals (Ni and V). <sup>c</sup>Microactivity = 100 – LCO – bottoms in ACE testing@527 °C, C/O = 6.

been found experimentally to follow a reaction order close to two.<sup>16</sup> The kinetic conversion, which results from integration of the second-order kinetic equation, is estimated by the expression<sup>44</sup>

$$\text{second order kinetic conversion} = \frac{\text{conversion}}{100 - \text{conversion}} \quad (1)$$

Catalysts B, C, and G were tested with the three H-Oil gas oils while catalyst C and D with the two commercial LNB feeds (20 wt % H-Oil gas oils/80 wt % SRVGO). Figure 3 shows a second order reaction plot for the 13 investigated cases, four catalysts, and five FCC feeds, suggesting that the catalytic cracking of the five feeds is well described by a second order reaction order. This is also supported by the high values of the squared correlation coefficient of regressions (Table 3). Table 3 also includes data about conversion values at the maximum C/O ratio of 7.3 wt/wt for easily discerning the catalyst activities and feed reactivities. The distinct values of the apparent second order kinetic constant along with the different conversion values at a catalyst to oil ratio of 7.3 wt/wt for the 13 cases indicate different reactivity of the studied FCC feeds and different activity of the tested catalysts. It was found in our earlier study that the reactivity of the H-Oil gas oils (HAGO, LVGO, and HVGO) strongly correlates with the Kw-factor,<sup>16</sup> with LVGO being characterized by the lowest Kw-factor.<sup>16</sup> The Kw-factor is a systematic way of classifying an oil according to its paraffinic, naphthenic, intermediate, or aromatic nature.<sup>45,46</sup> The Kw-factor in the range 12.5 to 13.0 indicates an oil of predominantly paraffinic constituents. The cyclic (naphthene) oils have a Kw-factor in the range 10.5 to 12.5, while the aromatic oils have a Kw-factor lower than 10.5.<sup>46</sup> The data in Table 3 confirm that the H-Oil LVGO has the lowest reactivity with the three tested catalysts B, C, and G. Catalyst B is the catalyst with the lowest second order kinetic constant, while catalysts C and G exhibit similar reactivity with all studied H-Oil gas oils.

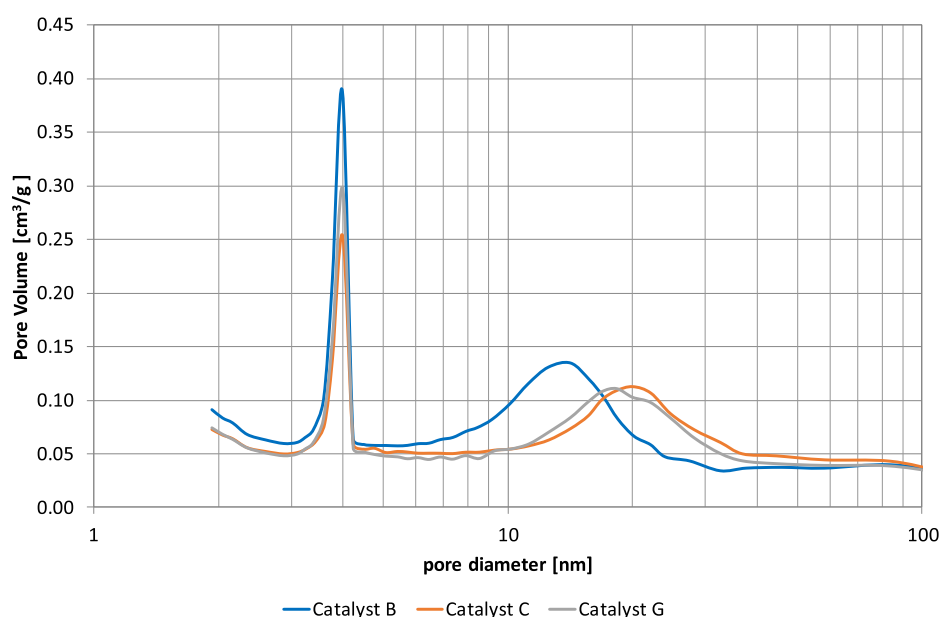


Figure 1. N<sub>2</sub> pore volume distribution of catalysts B, C, and G.

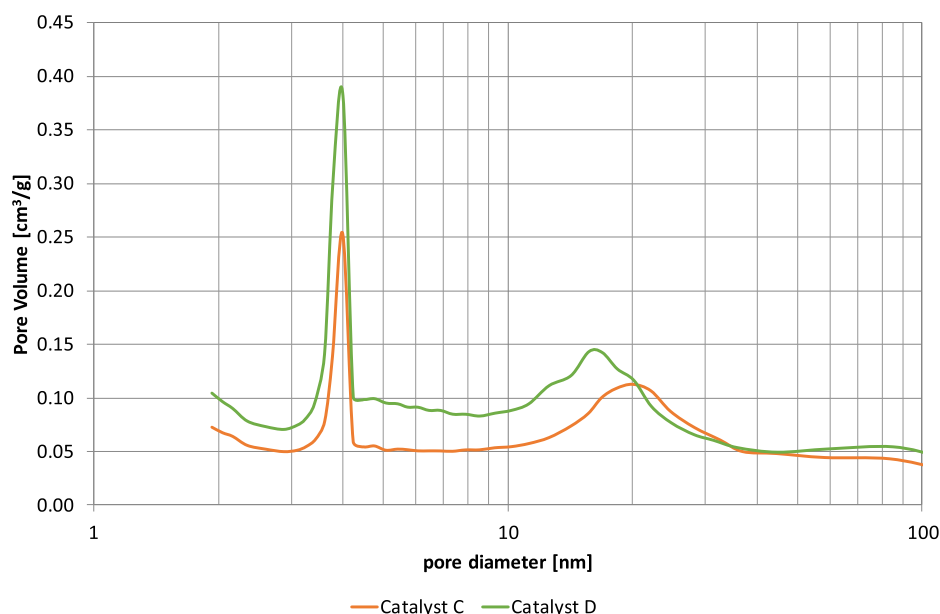


Figure 2. N<sub>2</sub> pore volume distribution of catalysts C and D.

The addition of 80 wt % SRVGO to the H-Oil VGO considerably improves the reactivity as evident from the values of the apparent second order kinetic constants for the feeds dated 06.12.2018 and 21.08.2019 (Table 3). With both feeds, catalyst C shows higher activity compared to catalyst D. However, catalyst C demonstrates higher  $\Delta$  coke. Catalyst  $\Delta$  coke, that is the difference between the coke on the spent catalyst and the coke on the regenerated catalyst, at a given reactor temperature and constant CO<sub>2</sub>/CO ratio, controls the regenerator temperature.<sup>47</sup> It is estimated by eq 2.

$$\text{Catalyst } \Delta \text{ coke} = \frac{\text{coke yield}}{\text{catalyst to oil ratio}} \quad (2)$$

The coke yield for a given commercial FCCU is essentially constant and mainly depends on the air blower capacity and/or availability of supplemental oxygen.<sup>47</sup> Therefore, the catalyst  $\Delta$

coke besides the regenerator temperature also controls the catalyst to oil ratio as evident from eq 2. When H-Oil gas oils are cracked, the maximum regenerator temperature limit can be surpassed if the catalyst has a higher  $\Delta$  coke selectivity.<sup>17</sup> Thus, the catalyst  $\Delta$  coke is of significant importance for the operation of commercial FCCUs—especially when H-Oil gas oils are cracked because of their greater affinity to make coke on the catalyst.<sup>17</sup> The  $\Delta$  coke for the 13 catalyst/feed combinations were therefore also calculated and reported in Table 3. With the three different H-Oil gas oils, catalysts C and G exhibit not only the same activity but also the same  $\Delta$  coke. With HAGO and HVGO, catalyst B shows a very low  $\Delta$  coke. However, when tested with the heaviest H-Oil HVGO feed, catalyst B demonstrates three times as high as  $\Delta$  coke relative to the  $\Delta$  coke of HAGO. This behavior cannot be seen with catalysts C and G. This finding is in line with that reported by

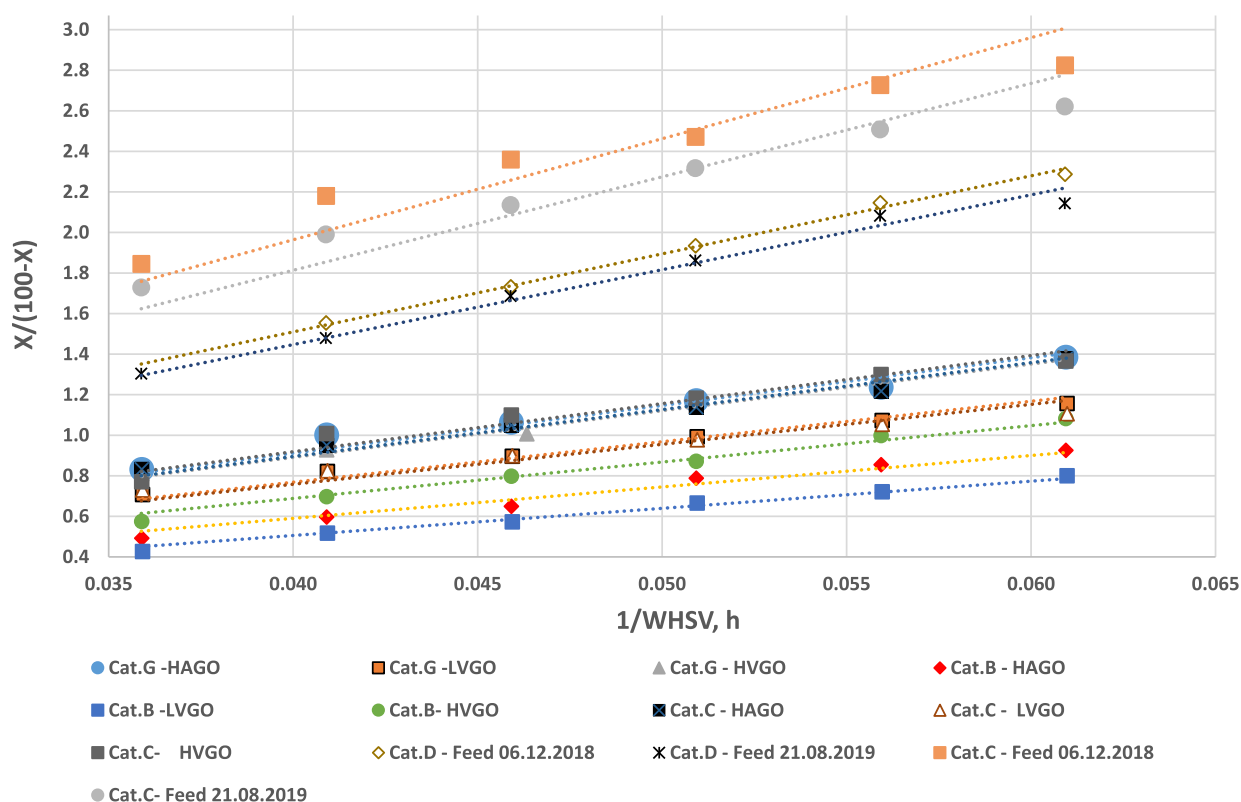


Figure 3. Second order kinetic plot for the studied catalysts and feeds.

Table 3. Values for the Apparent Second Order Kinetic Constant,  $R^2$ , and Catalyst Delta Coke for the 13 Catalyst/Feed Combinations Studied

Nr	H-Oil VGOs (LNB FCCU feeds)	apparent second order kinetic constant, $\text{frac.}^{-1} \text{h}^{-1}$	$R^2$	$\Delta$ coke, wt %	conversion, wt % ff at C/O = 7.3 wt/wt
1	Cat. G—HAGO	23.5	0.96	0.65	58.6
2	Cat. G—LVGO	20.0	0.98	0.80	54.3
3	Cat. G—HVGO	23.0	0.99	1.19	58.4
4	Cat. B—HAGO	15.5	0.97	0.33	48.8
5	Cat. B—LVGO	13.4	0.99	0.42	45.3
6	Cat. B—HVGO	18.0	0.98	1.03	52.6
7	Cat. C—HAGO	23.1	0.97	0.63	58.4
8	Cat. C—LVGO	19.7	0.90	0.78	53.2
9	Cat. C—HVGO	23.7	0.98	1.17	58.3
10	Cat. D—feed 06.12.2018 (LNB FCCU feed)	38.5	1.00	0.30	69.9
11	Cat. D—feed 21.08.2019 (LNB FCCU feed)	36.9	0.98	0.32	68.5
12	Cat. C—feed 06.12.2018 (LNB FCCU feed)	49.8	0.87	0.46	74.1
13	Cat. C—feed 21.08.2019 (LNB FCCU feed)	46.1	0.90	0.53	72.6

Harding et al.,<sup>48</sup> confirming that the catalyst performance is feedstock dependent.

It is interesting to note here that the difference between the activity of catalyst C and catalyst B, expressed by the ACE conversion at a CTO ratio of 7.3 wt/wt decreases in the following order: HAGO (9.6 wt %) > LVGO (7.9 wt %) > HVGO (5.7 wt %). The same difference for the catalyst G and B is as follows: HAGO (9.9 wt %) > LVGO (9.0 wt %) > HVGO (5.8 wt %). This finding suggests that the higher porosity of catalyst B relative to that of catalysts C and G renders lower diffusional constraints and the bigger H-Oil

VGO molecules concentrating in the LVGO and HVGO are easier to crack on this catalyst.

The catalyst  $\Delta$  coke difference between the catalysts C and B with the three H-Oil gas oils follows the order: LVGO (0.36 wt %) > HAGO (0.3 wt %) > HVGO (0.14 wt %). These results suggest that the coke selectivity is a function not only on the catalyst rare earth content as reported in the study of Haas and Nee<sup>49</sup> but also depends on the diffusional limitations as shown in our earlier research<sup>16</sup> and that of Kortunov et al.<sup>29</sup> When the highest molecular weight HVGO is cracked, the difference in the coke selectivity between the higher porosity catalyst B and the lower porosity catalysts C and G gets lower.

**Table 4. Product Yields at Constant Conversion of 48.3 wt % ff Corresponding to the H-Oil HAGO Cracking Experiment with Catalysts B, C, and G**

constant conversion = 48.3 wt % ff	dry gas, wt % ff	PPF, wt % ff	BBF, wt % ff	gasoline, wt % ff	LCO, wt % ff	HCO, wt % ff	coke, wt % ff
Cat. B (HAGO)	1.3	4.0	7.2	33.2	21.8	29.6	2.5
Cat. C (HAGO)	1.2	3.8	6.6	33.9	21.9	29.6	2.8
Cat. G (HAGO)	1.2	3.8	6.6	33.9	21.7	29.8	2.8

**Table 5. Product Yields at Constant Conversion of 48.3 wt % ff Corresponding to the H-Oil LVGO Cracking Experiment With Catalysts B, C, and G**

constant conversion = 48.3 wt % ff	dry gas, wt % ff	PPF, wt % ff	BBF, wt % ff	gasoline, wt % ff	LCO, wt % ff	HCO, wt % ff	coke, wt % ff
Cat. B (LVGO)	1.6	3.9	6.6	32.1	19.9	31.8	3.9
Cat. C (LVGO)	1.5	3.7	6.2	32.7	20.2	31.2	4.4
Cat. G (LVGO)	1.3	3.8	6.3	32.4	19.7	31.7	4.3

**Table 6. Product Yields at Constant Conversion of 48.3 wt % ff Corresponding to the H-Oil HVGO Cracking Experiment with Catalysts B, C, and G**

constant conversion = 48.3 wt % ff	dry gas, wt % ff	PPF, wt % ff	BBF, wt % ff	gasoline, wt % ff	LCO, wt % ff	HCO, wt % ff	coke, wt % ff
Cat. B (HVGO)	1.7	3.1	5.1	16.2	35.3	35.3	6.1
Cat. C (HVGO)	1.5	3.0	5.0	16.3	35.2	35.2	5.9
Cat. G (HVGO)	1.5	3.0	5.1	17.1	34.4	34.4	5.5

**Table 7. Product Yields at Constant Conversion of 67 wt % ff Corresponding to the LNB FCC Feed Dated 06.12.2018 with Catalysts C and D**

constant conversion = 67.0 wt % ff	dry gas, wt % ff	PPF, wt % ff	BBF, wt % ff	gasoline, wt % ff	LCO, wt % ff	HCO, wt % ff	coke, wt % ff
Cat. C (06.12.2018)	1.1	4.5	9.6	49.8	16.5	16.3	2.1
Cat. D (06.12.2018)	1.2	4.8	10.1	49.2	16.7	16.1	1.7

**Table 8. Product Yields at Constant Coke of 2.3 wt % ff Corresponding to the LNB FCC Feed Dated 06.12.2018 with Catalysts C and D**

constant coke yield = 2.3 wt % ff	dry gas, wt % ff	PPF, wt % ff	BBF, wt % ff	gasoline, wt % ff	LCO, wt % ff	HCO, wt % ff	coke, wt % ff
Cat. C (06.12.2018)	1.2	4.9	10.1	50.6	16.0	14.8	2.3
Cat. D (06.12.2018)	1.3	5.3	10.9	50.7	15.7	13.7	2.3

**Table 9. Product Yields at Constant Conversion of 67 wt % ff Corresponding to the LNB FCC Feed Dated 21.08.2019 with Catalysts C and D**

constant conversion = 67.0 wt % ff	dry gas, wt % ff	PPF, wt % ff	BBF, wt % ff	gasoline, wt % ff	LCO, wt % ff	HCO, wt % ff	coke, wt % ff
Cat. C (21.08.2019)	1.2	4.7	9.7	48.8	16.0	16.8	2.5
Cat. D (21.08.2019)	1.3	4.8	10.1	48.8	15.8	16.9	2.1

The probable reason for this finding may be because the difference between the size of the molecules of HVGO and LVGO and HAGO is much bigger than the difference in the porosity between the catalysts B and C (G).

In order to evaluate the catalyst product selectivity with the three H-Oil gas oils, the product yields were interpolated at constant conversion (48.3 wt % ff). Table 4 shows the interpolated data obtained by cracking the HAGO feed with catalysts B, C, and G. Catalysts C and G show very similar product selectivity. Catalyst B exhibits a higher LPG yield [75% of which is due to the higher butane–butylene fraction (BBF) yield] and lower gasoline yield. The bottom cracking is very similar with all three catalysts. Slightly lower coke yield is obtained with catalyst B with respect to catalysts C and G.

The product yields interpolated at constant conversion (48.3 wt % ff) relative to the LVGO cracking test—with catalysts B, C, and G—are reported in Table 5. Compared to catalyst C and G, catalyst B delivers slightly higher dry gas, higher BBF, slightly lower gasoline yield, and lower coke. As for HAVGO,

the three catalysts result in a similar bottom yield when tested with the LVGO feed.

Table 6 displays the product yield interpolation (constant conversion, 48.3 wt % ff) corresponding to the cracking of the HVGO feed with the same three catalysts (B, C, and G). With respect to catalyst C and G, catalyst B results in slightly higher dry gas and higher coke yield. Similar propane–propylene fraction (PPF), BBF, and gasoline yields are obtained with all three catalysts. With HVGO, catalyst G demonstrates the best performance in terms of the bottom cracking (lowest yield observed) and coke yield (lowest obtained). As mentioned later in this paper, bottom cracking was found to be the FCCU profitability driver. The data comparison at constant coke, which best relates to the catalyst performance that could be expected in a commercial FCCU, show catalyst B as the best performer with HAGO and LVGO feeds because of its better (lower) coke selectivity. However, with HVGO, catalyst G is expected to be the best performer because of its lowest coke make and best bottom cracking.

**Table 10. Product Yields at Constant Coke of 2.3 wt % ff Corresponding to the LNB FCC Feed Dated 21.08.2019 with Catalysts C and D**

constant coke yield = 2.3 wt % ff	dry gas, wt % ff	PPF, wt % ff	BBF, wt % ff	gasoline, wt % ff	LCO, wt % ff	HCO, wt % ff	coke, wt % ff
Cat. C (21.08.2019)	1.1	4.4	9.2	48.1	16.4	18.3	2.3
Cat. D (21.08.2019)	1.3	5.0	10.4	49.6	15.4	15.9	2.3

**Table 11. Product Yields Obtained at the LNB Commercial FCCU During Employment of Catalysts B and C and Processing the Same Feed**

constant coke = 4.4 wt % ff	dry gas, wt % ff	PPF, wt % ff	BBF, wt % ff	gasoline, wt % ff	LCO, wt % ff	HCO, wt % ff	SLO, wt % ff	coke, wt % ff
Cat. B (Nov.2016)	4.2	7.4	11.8	48.1	10.2	8.3	5.7	4.4
Cat. C (18.12.2018)	3.8	6.8	11.3	49.2	10.2	8.6	5.7	4.4

The product yields at constant conversion (67 wt %) for the cracking test of the LNB FCC feed dated 06.12.2018 with catalysts C and D are shown in Table 7. Catalyst C delivers less PPF and BBF yields but higher coke and gasoline yields. Similar dry gas and bottom yields are obtained with both catalysts. At constant coke yield (2.3 wt %, Table 8), catalyst D seems to perform better than catalyst C—given the higher PPF and BBF yields obtained, with similar gasoline yield and heavy cycle oil (HCO) yield.

Table 9 reports the product yields interpolated at constant conversion (67 wt % ff) relative to the cracking experiment of the LNB FCC feed dated 21.08.2019, tested with catalysts C and D. Similarly to what was observed with the LNB feed dated 06.12.2018, also with the 2019 LNB feed, catalyst C delivers higher coke yield and less BBF yield compared to catalyst D. The other product yields are very similar with both catalysts. At constant coke (2.3 wt %, Table 10), catalyst D shows better performance than catalyst C—as it results in higher yields of valuable products (PPF, BBF, and gasoline) and significantly lower bottom yield (−2.4 wt %  $\Delta$ ) than catalyst C.

The yield patterns of the catalysts can hereby be rationalized taking the porosity information as well as the acid site density into consideration. The lower acid site density of catalysts B and D results in a higher dominance of monomolecular cracking reactions suppressing secondary reactions which could contribute to higher coke formation.<sup>18,21</sup> Additionally, the higher porosity of catalysts B and D as reflected in the higher pore volumes (Table 2) as well as the nitrogen pore volume distributions (Figures 1, 2) enables an increased diffusion of the feed molecules to the acid sites of the catalyst and a faster egress of the cracking products. The latter minimizes secondary reaction contributions which are reported to increase coke yield.<sup>20</sup>

Based on the results of the laboratory cracking experiments, catalysts B and D would be the best candidates for FCCU operations with H-Oil/SRVGO blends—given the better coke selectivity. As shown in Figures 1 and 2, Catalyst B and catalyst D exhibit a higher pore volume in the mesoporous pore diameter range of 100–200 nm and higher nitrogen pore volume (Table 2). This higher porosity is reflecting improved diffusional properties of the catalysts to minimize secondary reactions that would result in increased delta coke and lower product olefinicities.<sup>43</sup>

By employing these catalysts in a commercial FCCU, higher yields of valuable products (PPF, BBF, and gasoline) and lower bottom yields would be expected. In order to verify these expectations based on laboratory cracking experiments, the catalytic performance of catalysts B and C was tested in the

LNB commercial FCCU, processing a feed with a similar quality as the one used for the laboratory tests. Table 11 summarizes the results of this comparison. Catalysts B and D show similar conversion as well as coke yield (4.4 wt %). Catalyst C delivers lower dry gas, PPF, and BBF yields and higher gasoline yield compared to catalyst B. The higher  $\Delta$  coke for catalyst C (0.66 wt % for catalyst C vs 0.58 wt % for catalyst B) resulted in an increase in regenerator temperature up to a point of the regenerator metallurgy temperature limit. Therefore, the FCCU was not capable of running up to the same high feed rate when catalyst C was employed. These results demonstrate that the catalyst performance expectations from the laboratory cracking tests are matched in the field—the lower coke selective catalysts B and D perform indeed better in the commercial FCCU. Additionally, this finding also highlights the importance in coke selectivity in FCC catalyst technology evaluation for the commercial FCCU's operation.

In order to assess the driving force for oil refining profitability improvement, the four catalysts evaluated in this study and another case involving the employment of a ZSM-5 additive in the amount of 2 wt % added to catalyst D were reckoned by the use of the LNB LP model and product yield distribution and product quality registered in the LNB FCCU during employment of the five catalytic systems.

In order to assess the refining profitability during employment of the four catalysts evaluated in this study, the yields and product quality during their use in the LNB refinery were put into the LNB LP model. Another additional case that included the use of catalyst D with 2 wt % ZSM-5 was evaluated, to judge the effect of ZSM-5 on the refinery economics. The reason to add ZSM-5 to catalyst D was to improve gasoline octane.<sup>50</sup> Table 12 presents a summary of the commercial LNB FCCU performance with the five cases mentioned above. It should be pointed out that this comparison is made only to define the driving force for the refinery profitability when different FCCU performances are judged. The fractionation of the gas oils light cycle oil (LCO), HCO, and SLO has not been absolutely the same for all five cases from Table 4. As determined from the laboratory experiments, the bottom cracking of all studied five cases was the same. Therefore, the different yields of gas oils for the five studied cases from Table 12 should be ascribed to the different fractionation efficiency of the LNB FCCU main fractionator registered during collecting the data, summarized in Table 12. By executing estimations for the refinery profitability by the use of the LNB LP model employing Honeywell RPMS (Refining and Petrochemical Modelling System) software and employing intercriteria analysis (ICrA), it was found that the single factor that mostly

**Table 12. Yields and Product Quality During the Use of the Four Studied Catalysts in the Commercial LNB FCC Unit**

yields, and product quality	Cat. B	Cat. C	Cat. D	Cat. D + 2 wt % ZSM-5	Cat. G
	Yields, wt % ff				
dry gas	4.6	3.8	4.4	4.4	4.3
PPF	7	6.8	6.7	8.3	6.9
BBF	11.5	11.3	11.1	12.6	10.8
gasoline	41.9	44.5	44.3	41.5	44.2
LCO	10.4	10.5	10.0	10.0	10.3
HCO	7.5	6.9	6.5	6.3	7.1
SLO	12.7	11.7	12.5	12.5	12.1
coke	4.3	4.4	4.4	4.3	4.2
losses	0.1	0.1	0.1	0.1	0.1
	Product Quality				
content of iso-C4= in BBF, vol %	19.4	16.1	18.8	20.9	16.1
content of iso-C4 in BBF, vol %	31.1	31.7	30.5	28.4	34.4
RON	94.0	93.4	94.0	94.0	93.8
MON	82.0	81.8	82.0	82.1	82.0
conversion, wt % ff	69.3	70.8	70.9	71.1	70.4
Δ coke, wt %	0.59	0.67	0.58	0.58	0.66
catalyst to oil ratio, wt/wt	7.3	6.6	7.6	7.4	6.4

affects refining profitability is the extent of bottoms of the barrel upgrading estimated by the following equation

$$\text{EBBU} = \frac{\text{crude} - \text{FO} - \text{losses}}{\text{crude}} \quad (3)$$

where EBBU = extent of the bottoms of the barrel upgrading, wt %. Crude = the amount of crude processed in the refinery, t/h. FO = the amount of fuel oil produced in the refinery, t/h. Losses = the amount of losses during petroleum refining, t/h.

Figure 4 shows graphs of the relation of refining margin to the EBBU and the relation of FCC SLO yield to the EBBU. It is clear from these data that the SLO yield is the biggest single factor that mostly affects the economics of the FCCU operation. It should be mentioned here that the LNB FCCU SLO yield can be considered equivalent to the HCO yield from the laboratory ACE unit because they have similar distillation characteristics. The LNB FCCU SLO is the fraction boiling >360 °C, while the LNB FCCU HCO is the fraction boiling in the range 300–360 °C, and the LCO is the fraction boiling in the range 200 (210)–300 °C.

The ICRA revealed that the refining margins are statistically meaningful negatively weakly affected by FCC dry gas production and weakly positively affected by gasoline production. However, the FCC SLO production is strongly negatively related to the refining margin outweighing in its significance in the effects of both gasoline and dry gas production. The use of ZSM-5 as evident from the data in Table 12 led to increasing of both PPF (+1.6 wt % ff) and BBF (+1.5 wt % ff) at the expense of decreasing the gasoline yield (−2.8 wt % ff) without any octane improvement. Obviously, for the conditions studied (crude oil, product prices, utility costs of November 2020), this change in the yields, a result from ZSM-5 action, had no effect on the economics of the commercial FCCU operation because it did not influence the FCC SLO yield.

The data in Table 2 also show that during the employment of the five catalytic systems, the commercial LNB FCCU has operated at a constant coke yield of  $4.3 \pm 0.1$  wt % ff. Comparing the conversion levels and the catalyst to oil ratios

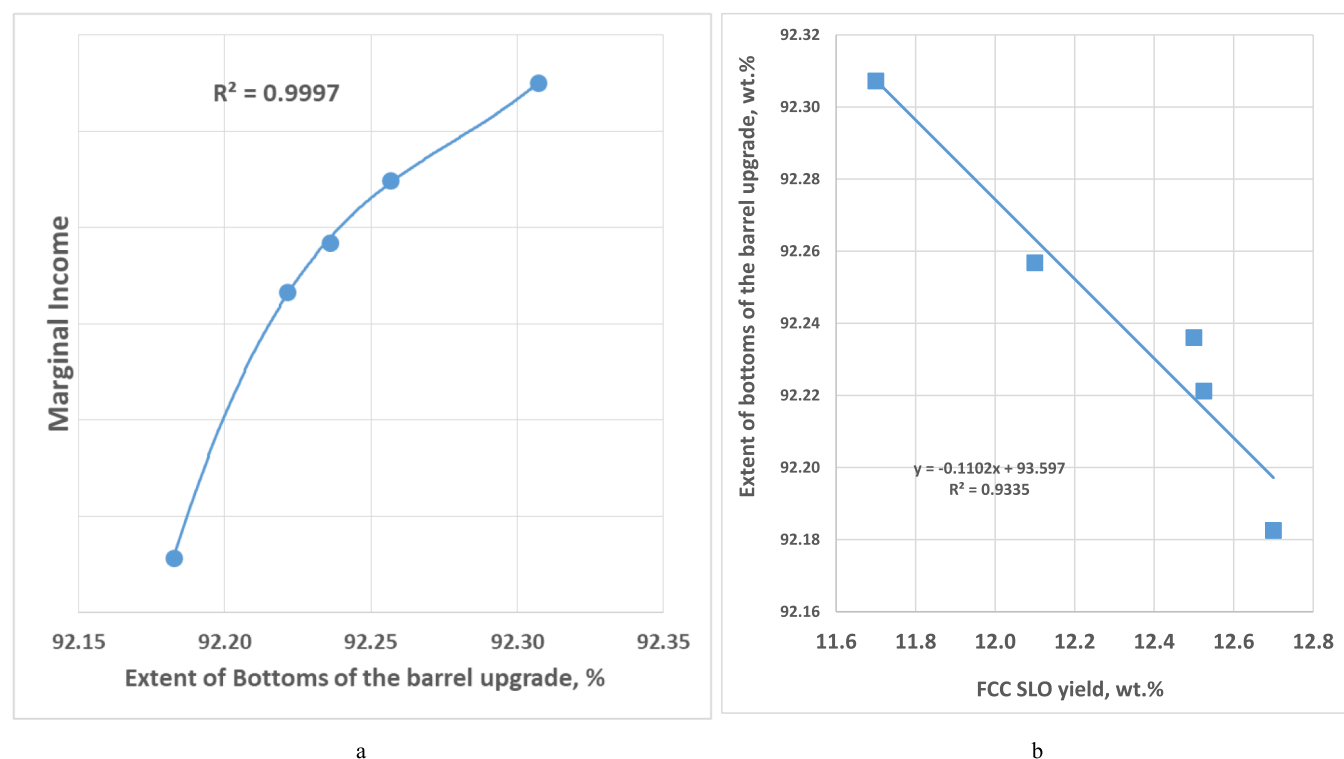


**Figure 4.** Correlation between (a) EBBU and refining margin and between (b) EBBU and FCC SLO yield.



for the five investigated cases from Table 12, one can see that they are variable. Therefore, a conclusion can be made that catalyst performance evaluation in laboratory catalytic cracking units that best emulates the real world commercial FCCU performance is that at constant coke yield. Neither a constant C/O ratio nor constant conversion can give a real notion of what would be the performance of any catalyst–feedstock combination in the commercial FCCU. It is evident from the data in Table 12 that  $\Delta$  coke of catalysts C and G is higher what can be tolerated by a regenerator metallurgical limit of 0.64 wt %. Therefore, lower throughput or excluding the H-Oil HVGO from the FCC feed slate is needed to comply with the regenerator metallurgical limitations. That was exactly what happened at the LNB FCCU. Regardless of the higher activity of catalysts C and G demonstrated in the ACE laboratory FCCU (see Table 3), their performance in the commercial LNB FCCU during processing H-Oil gas oils limited the flexibility in the selection of the most profitable way of utilization of the different H-Oil gas oils. The synergy between both conversion processes, the ebullated bed VR hydrocracking and the FCC leading to a higher petroleum refining profitability, can be improved when the FCC catalyst with properly designed characteristics is used. Alleviating the diffusional constraints of FCC catalysts can decrease the coke make selectivity that along with a higher activity can bring a higher conversion and low SLO yield, that eventually leads to a better oil refining economics.

The better coke selectivity of catalysts B and D and their better performance observed at constant coke make in the ACE laboratory FCCU suggest a better performance of these catalysts in the commercial LNB FCCU. In fact, the operation of these catalysts in the commercial LNB FCCU gave a higher degree of freedom when opportunity appeared to gain from a higher throughput operation. Therefore, the preliminary catalyst testing in laboratory and pilot plants can discover which catalyst can deliver better profitability, and such a test requires a small amount of time. However, the catalyst test in a commercial FCCU may take about four months to replace the incumbent catalyst from the unit inventory, and in case of a poor performance of the new catalyst candidate, the losses of profit opportunity could be huge. The ACE tests can give a notion about the feasible performance of a given catalyst in a commercial FCCU. However, as observed in this study, the difference in the  $\Delta$  coke between the studied catalysts was much bigger in the ACE unit (0.21 wt %) than that registered at the commercial FCCU (0.09 wt %). Moreover, the higher dispersion of coke yield measurement at the ACE unit accounting for a relative error of about 10%<sup>16</sup> can be the reason for overestimation or underestimation of any catalyst performance compared at constant coke yield. The riser circulating pilot plant seems to be the best candidate for preliminary catalyst selection tests because it closest emulates the performance of the real world commercial FCCU.<sup>51,52</sup> Other laboratory catalytic cracking units like the riser simulator (batch fluidized bed)<sup>53,54</sup> and micro down flow unit<sup>55,56</sup> have also reported results showing a very close simulation of the circulating riser performance. They could be also used for preliminary catalyst selection tests after proving that their performance perfectly matches the real world commercial FCCU performance.

## ■ CONCLUSIONS

The performance of three catalysts—labeled as B, C, and G—has been evaluated in laboratory cracking experiments with H-Oil gas oils—HAGO, LVGO, and HVGO (with LVGO being characterized by the lowest Kw). With all three catalysts, HAGO and HVGO exhibit very similar reactivity. HVGO makes much more delta coke than HAGO, double as high, with catalysts C and G and three times as high when catalyst B is tested. This highlights that the balance of catalyst porosity and acid site density play a decisive role in catalyst design for these secondary gas oil streams. Catalyst B would be the preferable choice for implementation in commercial FCCUs processing H-Oil LVGO and HAGO, given its better coke selectivity. In combination with H-Oil HVGO, catalyst B shows however highest coke selectivity. Based on both ACE cracking experimental results and the commercial FCCU performance results, it could be concluded that the lower activity and the lower coke selectivity catalyst is a better choice for employment in the commercial FCCU. However, the laboratory ACE cracking experimental results at constant coke indicate much better performance than that observed in the commercial FCCU. Therefore, the comparisons of product yields at constant coke obtained by testing different catalysts in laboratory cracking experiments could be considered indicative but not precise for the use in the process of catalyst evaluation applying a refinery LP model. The LNB refinery LP model employing the Honeywell RPMS software and using the data generated by employing four catalysts and one catalyst plus ZSM-5 additive revealed that the predominant factor that controls refinery profitability related to the FCCU performance is the FCC SLO yield. The lower the FCC SLO yield, the better the refinery economics. All other factors like the other product yields and product qualities, except the FCC SLO yield for the conditions studied, are suppressed by the dominant effect of the FCC SLO yield.

## ■ EXPERIMENTAL SECTION

The properties of the two LNB commercial feeds as well as of the three H-Oil gas oils used to perform the cracking experiments are reported in Table 1. Among the three H-Oil gas oils, HVGO oil is characterized by the highest density, followed by LVGO and HAGO. The three feeds differ also in terms of Conradson carbon and sulfur content. Compared to HAGO and LVGO, the HVGO oil has the highest Conradson carbon value— $\sim 2$  wt %. HVGO is also characterized by a higher S level (0.67 wt %) with respect to HAGO (0.37 wt %) and LVGO (0.48 wt %). In terms of composition, HAGO contains a higher fraction of paraffins (50.7 wt %) compared to HVGO (48.6 wt %) and LVGO (47.6 wt %). A similar trend is also observed for the naphthene level, which decreases in the order HAGO > HVGO > LVGO. Accordingly, the opposite trend is seen for the aromatic portion of the feeds (HAGO < HVGO < LVGO). Regarding the two LNB commercial feeds, compared to the 2018 feed, the one dated 2019 shows a slight increase in density, refractive index, and Conradson carbon content as well as an increase in boiling point distribution. The sulfur content and basic nitrogen are slightly lower. Aromatic content of the 2019 feed is also higher.

The catalytic properties were determined with an advanced cracking evaluation (ACE) pilot plant at six different catalyst-to-oil ratios (C/O) ranging from 4.3 to 7.3 g/g to generate conversion and yield response curves. The C/O ratios were

varied by changing the mass of the catalyst while keeping the feed amount and the feed time on stream constant, at 1.5 g and 30 s, respectively. The catalyst bed temperature was adjusted at 527 °C. Chromatographic methods were employed for analysis of the gas and liquid products obtained from the cracking experiments and to determine the gasoline research octane number (RON) and motor octane numbers (MON).<sup>42</sup> The octane numbers (RON and MON) were calculated by means of a proprietary octane model, which takes into account nonlinear blending characteristics of hydrocarbons contained in FCC gasoline.<sup>42</sup> The fractions of gasoline, LCO, and HCO were determined at cut points of 221 °C (gasoline/LCO) and 338 °C (LCO/HCO). The carbon amount left on the catalyst after the tests was determined by means of a carbon analyzer. The yields were calculated as the weight percent of the reactant, while the conversion was estimated as

$$\text{conversion, wt \% fresh feed} = 100 - \text{LCO} - \text{HCO} \quad (4)$$

The weight hourly space velocity has been estimated by the equation

$$\text{WHSV} = \frac{3600}{\text{C/O} \cdot \text{TOS}} \quad (5)$$

where WHSV = weight hourly space velocity, h<sup>-1</sup>; C/O = catalyst-to-oil ratio, g/g; and TOS = catalyst time on stream (30 s in our case).

More details about the employed ACE unit can be found in ref 25.

## AUTHOR INFORMATION

### Corresponding Author

Dicho Stratiev – LUKOIL Neftohim Burgas, 8104 Burgas, Bulgaria; [orcid.org/0000-0001-7486-0589](https://orcid.org/0000-0001-7486-0589);  
Email: [stratiev.dicho@neftochim.bg](mailto:stratiev.dicho@neftochim.bg)

### Authors

Ivelina Shishkova – LUKOIL Neftohim Burgas, 8104 Burgas, Bulgaria; [orcid.org/0000-0002-3959-9095](https://orcid.org/0000-0002-3959-9095)

Mihail Ivanov – LUKOIL Neftohim Burgas, 8104 Burgas, Bulgaria

Rosen Dinkov – LUKOIL Neftohim Burgas, 8104 Burgas, Bulgaria; [orcid.org/0000-0002-9772-1845](https://orcid.org/0000-0002-9772-1845)

Borislav Georgiev – LUKOIL Neftohim Burgas, 8104 Burgas, Bulgaria

Georgi Argirov – LUKOIL Neftohim Burgas, 8104 Burgas, Bulgaria

Vassia Atanasova – Institute of Biophysics and Biomedical Engineering, Bulgarian Academy of Sciences, 1113 Sofia, Bulgaria

Petar Vassilev – Institute of Biophysics and Biomedical Engineering, Bulgarian Academy of Sciences, 1113 Sofia, Bulgaria

Krassimir Atanasov – Institute of Biophysics and Biomedical Engineering, Bulgarian Academy of Sciences, 1113 Sofia, Bulgaria; University Prof. Dr. Assen Zlatarov, 8010 Burgas, Bulgaria

Dobromir Yordanov – University Prof. Dr. Assen Zlatarov, 8010 Burgas, Bulgaria

Aleksey Popov – Grace CIS, Moscow 125047, Russian Federation

Alessia Padovani – Grace GmbH, 67547 Worms, Germany

Ulrike Hartmann – Grace GmbH, 67547 Worms, Germany

Stefan Brandt – Grace GmbH, 67547 Worms, Germany;

[orcid.org/0000-0003-4365-5077](https://orcid.org/0000-0003-4365-5077)

Svetoslav Nenov – University of Chemical Technology and Metallurgy, 1756 Sofia, Bulgaria

Sotir Sotirov – University Prof. Dr. Assen Zlatarov, 8010 Burgas, Bulgaria

Evdokia Sotirova – University Prof. Dr. Assen Zlatarov, 8010 Burgas, Bulgaria

Complete contact information is available at:

<https://pubs.acs.org/10.1021/acsomega.0c06207>

## Notes

The authors declare no competing financial interest.

## ACKNOWLEDGMENTS

The authors Vassia Atanasova, P.V., Krassimir Atanasov, S.S., and Evdokia Sotirova acknowledge the support from the project UNITE BG05M2OP001-1.001-0004/28.02.2018 (2018–2023).

## ABBREVIATIONS

ACE, advanced cracking evaluation

BBF, butane–butylene fraction

C\_Aromatics, aromatic carbon content (estimated by n-d-M method, ASTM D3238)

C\_Naphthenes, naphthenic carbon content (estimated by n-d-M method, ASTM D3238)

C\_Paraffins, paraffinic carbon content (estimated by n-d-M method, ASTM D3238)

CN, cracked naphtha (gasoline)

C/O, catalyst-to-oil ratio

EBBU, extent of the bottoms of the barrel upgrading

FCC, fluid catalytic cracking

FCCU, fluid catalytic cracking unit

ff, fresh feed

FO, fuel oil

HAGO, heavy atmospheric gas oil

HCO, heavy cycle oil

HVGO, heavy vacuum gas oil

LCO, light cycle oil

LNB, LUKOIL Neftohim Burgas refinery, Bulgaria

LVGO, light vacuum gas oil

LP, linear programming

PPF, propane–propylene fraction

PV, pore volume

SLO, slurry oil

SRVGO, straight run VGO

TOS, catalyst time on stream

UCS, unit cell size

VGO, vacuum gas oil

VR, vacuum residue

WHSV, weight hourly space velocity

wt % ff, weight percent of fresh feed processed

## REFERENCES

(1) Vogt, E. T. C.; Weckhuysen, B. M. Fluid Catalytic Cracking: Recent Developments on the Grand Old Lady of Zeolite Catalysis. *Chem. Soc. Rev.* **2015**, *44*, 7342–7370.

(2) Bai, P.; Etim, U. J.; Yan, Z.; Mintova, S.; Zhang, Z.; Zhong, Z.; Gao, X. Fluid Catalytic Cracking Technology: Current Status and Recent Discoveries on Catalyst Contamination. *Catal. Rev.* **2019**, *61*, 333–405.

- (3) Tian, Y.; Che, Y.; Chen, M.; Feng, W.; Zhang, J.; Qiao, Y. Catalytic Upgrading of Vacuum Residue-Derived Cracking Gas-Oil for Maximum Light Olefin Production in a Combination of a Fluidized Bed and Fixed Bed Reactor. *Energy Fuels* **2019**, *33*, 7297–7304.
- (4) Liu, Y.; An, Z.; Yan, H.; Chen, X.; Feng, X.; Tu, Y.; Yang, C. Conceptual Coupled Process for Catalytic Cracking of High-Acid Crude Oil. *Ind. Eng. Chem. Res.* **2019**, *58*, 4794–4801.
- (5) Al-Khattaf, S.; Saeed, M. R.; Aitani, A.; Klein, M. T. Catalytic Cracking of Light Crude Oil to Light Olefins and Naphtha over E-Cat and MFI: Microactivity Test versus Advanced Cracking Evaluation and the Effect of High Reaction Temperature. *Energy Fuels* **2018**, *32*, 6189–6199.
- (6) Al-Absi, A. A.; Al-Khattaf, S. S. Conversion of Arabian Light Crude Oil to Light Olefins via Catalytic and Thermal Cracking. *Energy Fuels* **2018**, *32*, 8705–8714.
- (7) Al-Sabawi, M.; Chen, J.; Ng, S. Fluid Catalytic Cracking of Biomass-Derived Oils and Their Blends with Petroleum Feedstocks: A Review. *Energy Fuels* **2012**, *26*, 5355–5372.
- (8) Corma, A.; Huber, G.; Sauvanaud, L.; O'connor, P. Processing Biomass-Derived Oxygenates in the oil Refinery: Catalytic Cracking (FCC) Reaction Pathways and Role of Catalyst. *J. Catal.* **2007**, *247*, 307–327.
- (9) Ajibola, A. A.; Omoleye, J. A.; Efeovbokhan, V. E. Catalytic Cracking of Polyethylene Plastic Waste Using Synthesised Zeolite Y from Nigerian Kaolin Deposit. *Appl. Petrochem. Res.* **2018**, *8*, 211–217.
- (10) Fisher, I. P. Effect of Feedstock Variability on Catalytic Cracking yields. *Appl. Catal.* **1990**, *65*, 189–210.
- (11) Navarro, U.; Ni, M.; Orlicki, D. Understanding the Potential for FCC Feed to Generate Valuable Products and How This Knowledge Can Benefit Refinery Operation. PTQ, 2015. [www.digitalrefining.com/article/1001054](http://www.digitalrefining.com/article/1001054).
- (12) Stratiev, D.; Shishkova, I.; Veli, A.; Nikolova, R.; Stratiev, D. D.; Mitkova, M.; Yordanov, D. Fluid Catalytic Cracking and Thermal Cracking of Vacuum Gas Oils. Effect of Feedstock Properties on Conversion and Yields. *OGEM* **2017**, *2*, 84–89.
- (13) Wang, G.; Liu, Y.; Wang, X.; Xu, C.; Gao, J. Studies on the Catalytic Cracking Performance of Coker Gas Oil. *Energy Fuels* **2009**, *23*, 1942–1949.
- (14) Li, Z.; Wang, G.; Gao, J. Effect of Retarding Components on Heavy Oil Catalytic Cracking and Their Corresponding Countermeasures. *Energy Fuels* **2019**, *33*, 10833–10843.
- (15) Li, Z.-k.; Wang, G.; Shi, Q.; Xu, C.-m.; Gao, J.-s. Retardation Effect of Basic Nitrogen Compounds on Hydrocarbons Catalytic Cracking in Coker Gas Oil and Their Structural Identification. *Ind. Eng. Chem. Res.* **2011**, *50*, 4123–4132.
- (16) Stratiev, D.; Shishkova, I.; Ivanov, M.; Dinkov, R.; Georgiev, B.; Argirov, Atanassova, V.; Vassilev, P.; Atanassov, K.; Yordanov, D.; Popov, A.; Padovani, A.; Hartmann, U.; Nenov, S. Catalytic cracking of diverse vacuum residue hydrocracking gas oils. *Chem. Eng. Technol.* **2021**, in press. DOI: 10.1002/ceat.202000577.
- (17) Stratiev, D.; Shishkova, I.; Ivanov, M.; Chavdarov, I.; Yordanov, D. Dependence of Fluid Catalytic Cracking Unit Performance on H-Oil Severity, Catalyst Activity, and Coke Selectivity. *Chem. Eng. Technol.* **2020**, *43*, 2266–2276.
- (18) Bryden, K.; Singh, U.; Berg, M.; Brandt, S.; Schiller, R.; Cheng, W. C. Fluid Catalytic Cracking (FCC): Catalysts and Additives. *Kirk-Othmer Encyclopedia of Chemical Technology*; John Wiley & Sons, 2015.
- (19) Velthoen, M. E. Z. Lewis Acidity in Cracking and Polymerization Catalysts. Ph.D. Thesis, University Utrecht, 2019.
- (20) Wu-Cheng, C.; Habib, E. T.; Rajagopalan, K.; Roberie, T. G.; Wormsbecher, R. F.; Ziebarth, M. S. In *Fluid Catalytic Cracking in Handbook of Heterogeneous Catalysis*, 2nd ed.; Ertl, G., Knözinger, H., Schüth, F., Weitkamp, J., Eds.; Wiley-VCH Verlag: Weinheim, 2008; pp 2741–2778.
- (21) Wallenstein, D.; Fougret, C.; Brandt, S.; Hartmann, U. Application of Inverse Gas Chromatography for Diffusion Measurements and Evaluation of Fluid Catalytic Cracking Catalysts. *Ind. Eng. Chem. Res.* **2016**, *55*, 5526–5535.
- (22) García, J. R.; Falco, M.; Sedran, U. Impact of the desilication treatment of Y zeolite on the catalytic cracking of bulky hydrocarbon molecules. *Top. Catal.* **2016**, *59*, 268–277.
- (23) Falco, M.; Morgado, E.; Amadeo, N.; Sedran, U. Accessibility in alumina matrices of FCC catalysts. *Appl. Catal., A* **2006**, *315*, 29–34.
- (24) García, J. R.; Falco, M.; Sedran, U. Intracrystalline mesoporosity over Y zeolites. Processing of VGO and resid-VGO mixtures in FCC. *Catal. Today* **2017**, *296*, 247–253.
- (25) Fals, J.; García, J. R.; Falco, M.; Sedran, U. Performance of Equilibrium FCC Catalysts in the Conversion of the SARA Fractions in VGO. *Energy Fuels* **2020**, *34*, 16512–16521.
- (26) Fals, J.; García, J. R.; Falco, M.; Sedran, U. Coke from SARA fractions in VGO. Impact on Y zeolite acidity and physical properties. *Fuel* **2018**, *225*, 26–34.
- (27) Al-Khattaf, S.; de Lasa, H. Activity and Selectivity of Fluidized Catalytic Cracking Catalysts in a Riser Simulator: The Role of Y-Zeolite Crystal Size. *Ind. Eng. Chem. Res.* **1999**, *38*, 1350–1356.
- (28) Atias, J. A.; de Lasa, H. Adsorption, Diffusion, and Reaction Phenomena on FCC Catalysts in the CREC Riser Simulator. *Ind. Eng. Chem. Res.* **2004**, *43*, 4709–4720.
- (29) Kortunov, P.; Vasenkov, S.; Kärger, J.; Fé Elía, M.; Perez, M.; Stöcker, M.; Papadopoulos, G. K.; Theodorou, D.; Drescher, B.; McElhiney, G.; et al. Diffusion in Fluid Catalytic Cracking Catalysts on Various Displacement Scales and Its Role in Catalytic Performance. *Chem. Mater.* **2005**, *17*, 2466–2474.
- (30) Stratiev, D.; Dinkov, R.; Shishkova, I.; Sharafutdinov, I.; Ivanova, N.; Mitkova, M.; Yordanov, D.; Rudnev, N.; Stanulov, K.; Artemiev, A.; Barova, I.; Chushkov, B. What is Behind the High Values of Hot Filtration Test of the Ebullated Bed Residue H-Oil Hydrocracker Residual Oils? *Energy Fuels* **2016**, *30*, 7037–7054.
- (31) Stratiev, D.; Nenov, S.; Shishkova, I.; Georgiev, B.; Argirov, G.; Dinkov, R.; Yordanov, D.; Atanassova, V.; Vassilev, P.; Atanassov, K. Commercial Investigation of the Ebullated-Bed Vacuum Residue Hydrocracking in the Conversion Range of 55–93. *ACS Omega* **2020**, *5*, 33290.
- (32) Zepeda, H. M. P. Novel Mesoporous Catalysts for Vacuum Residue Hydrocracking. Ph.D. Thesis, Imperial College London, 2013.
- (33) Miki, Y.; Yamadaya, S.; Oba, M.; Sugimoto, Y. Role of Catalyst in Hydrocracking of Heavy Oil. *J. Catal.* **1983**, *83*, 371–383.
- (34) Manek, E.; Haydary, J. Hydrocracking of vacuum residue with solid and dispersed phase catalyst: Modeling of sediment formation and hydrodesulfurization. *Fuel Process. Technol.* **2017**, *159*, 320–327.
- (35) Martínez, J.; Sánchez, J. L.; Ancheyta, J.; Ruiz, R. S. A Review of Process Aspects and Modeling of Ebullated Bed Reactors for Hydrocracking of Heavy Oils. *Catal. Rev.: Sci. Eng.* **2010**, *52*, 60–105.
- (36) Ancheyta, J. *Modeling of Processes and Reactors for Upgrading of Heavy Petroleum*; Taylor & Francis Group: Boca Raton, FL, 2013; pp 33487–42742.
- (37) Stratiev, D.; Shishkova, I.; Yankov, V.; Kolev, I.; Mitkova, M. Impact of H-Oil vacuum residue hydrocracking severity on fluid catalytic cracking unit performance. *Pet. Sci. Technol.* **2020**, *38*, 565–573.
- (38) Stratiev, D.; Shishkova, I.; Dinkov, R.; Yordanov, D. Studying of the processing of fluid catalytic cracking slurry oil in the H-Oil ebullated bed vacuum residue hydrocracking and its effect on the H-Oil vacuum gas oil quality and fluid catalytic cracking performance. *Pet. Coal* **2020**, *62*, 542–556.
- (39) Kam, E. K. T.; Al-Mashan, M. H.; Al-Azmi, H. The Mixing Aspects of NiMo and CoMo Hydrotreating Catalysts in Ebullated-Bed Reactors. *Catal. Today* **1999**, *48*, 229–236.
- (40) Kam, E. K. T.; Jasam, F.; Al-Mashan, M. Catalyst Attrition in Ebullated-Bed Hydrotreater Operations. *Catal. Today* **2001**, *64*, 297–308.
- (41) Melin, M.; Brandt, S.; Baillie, C.; McQueen, D. The Importance of Using Pilot Plant Testing for FCC Catalyst Selection, PTQ, 2013. <http://www.digitalrefining.com/article/1000767>.

(42) Mitkova, M.; Stratiev, D.; Shishkova, I.; Dobrev, D. *Thermal and Thermo-Catalytic Processes for Heavy Oil Conversion*; Professor Marin Drinov Publishing House of Bulgarian Academy of Sciences: Sofia, 2017.

(43) Wallenstein, D.; Schäfer, K.; Harding, R. H. Impact of Rare Earth Concentration and Matrix Modification in FCC Catalysts on Their Catalytic Performance in a Wide Array of Operational Parameters. *Appl. Catal., A* **2015**, *502*, 27–41.

(44) Lappas, A. A.; Iatridis, D. K.; Kopalidou, E. P.; Vasalos, I. A. Influence of Riser Length of a Fluid Catalytic Cracking Pilot Plant on Catalyst Residence Time and Product Selectivity. *Ind. Eng. Chem. Res.* **2017**, *56*, 12927–12939.

(45) Gharagheizi, F.; Fazeli, A. Prediction of the Watson Characterization Factor of Hydrocarbon Components from Molecular Properties. *QSAR Comb. Sci.* **2008**, *27*, 758–767.

(46) Kaiser, M. J.; De Klerk, A.; Gary, J. H.; Handwerk, G. E. *Petroleum Refining. Technology, Economics, and Markets*, 6ed; CRC Press: Boca Raton, FL, 2020.

(47) Sadeghbeigi, R. *Fluid Catalytic Cracking Handbook An Expert Guide to the Practical Operation, Design, and Optimization of FCC Units*, 4 ed.; Elsevier: Cambridge, MA, 2020.

(48) Harding, R. H.; Zhao, X.; Deady, J. *Cracking FCC paradims: Part one catalyst performance is feedstock dependent*; NPRA Annual Meeting, San Antonio, Texas, AM-97-31, 1997.

(49) Haas, A.; Nee, J. The role of zeolite and matrix activity in FCC catalysts on the molecular weight distribution of vacuum gas oil cracking products. *Erdoel, Erdgas, Kohle* **1996**, *7*, 312–314.

(50) Degnan, T. F.; Chitnis, G. K.; Schipper, P. H. History of ZSM-5 fluid catalytic cracking additive development at Mobil. *Microporous Mesoporous Mater.* **2000**, *35–36*, 245–252.

(51) Young, G. W.; Weatherbee, G. D. *FCCU Studies with an Adiabatic Circulating Pilot Unit*, AIChE, Annual Meeting, San Francisco, November 1989.

(52) Lappas, A. A.; Iatridis, D. K.; Papapetrou, M. C.; Kopalidou, E. P.; Vasalos, I. A. Feedstock and catalyst effects in fluid catalytic cracking - Comparative yields in bench scale and pilot plant reactors. *Chem. Eng. J.* **2015**, *278*, 140–149.

(53) Sedran, U. A. Laboratory Testing of FCC Catalysts and Hydrogen Transfer Properties Evaluation. *Catal. Rev.: Sci. Eng.* **1994**, *36*, 405–431.

(54) Passamonti, F.; de la Puente, G.; Gilbert, W.; Morgado, E.; Sedran, U. Comparison between fixed fluidized bed (FFB) and batch fluidized bed reactors in the evaluation of FCC catalysts. *Chem. Eng. J.* **2012**, *183*, 433–447.

(55) Corma, A.; Martínez, C.; Melo, F. V.; Sauvanaud, L.; Carriat, J. Y. A new continuous laboratory reactor for the study of catalytic cracking. *Appl. Catal., A* **2002**, *232*, 247–263.

(56) Corma, A.; Sauvanaud, L. FCC testing at bench scale: New units, new processes, new feeds. *Catal. Today* **2013**, *218–219*, 107–114.